

A quantum byte with 10^{-5} cross-talk for fault-tolerant quantum computing

Ch. Piltz, Th. Sriarunothai, A. F. Varón, and Ch. Wunderlich

Department Physik, Naturwissenschaftlich-Technische Fakultät, Universität Siegen, 57068 Siegen, Germany

(Dated: 28 March 2014)

The addressing of a particular qubit within a quantum register is a key prerequisite for scalable quantum computing. We demonstrate addressing of individual qubits within a quantum byte (eight qubits) and measure the error induced in non-addressed qubits (cross-talk) associated with the application of single-qubit gates. This cross-talk is on the order of 10^{-5} breaching the threshold for fault-tolerant quantum computing. The quantum byte is implemented using $^{171}\text{Yb}^+$ ions confined in a Paul trap where a static magnetic gradient field is applied that lifts the hyperfine qubits' degeneracy. Hyperfine qubits are individually addressed using microwave radiation. In addition, we demonstrate a method for addressing individual qubits where an appropriate choice of addressing frequency and microwave pulse duration allows for further lowering cross-talk.

The precise control of quantum systems is a key ingredient for the realization of quantum information processing devices such as a quantum computer. The level of quantum control achieved with trapped ion based systems is still unsurpassed. Yet, scaling up such a system to enable large-scale quantum computing is a major challenge. If the gate errors could be made small enough, then the application of quantum error correction protocols would make scalable fault-tolerant quantum computation possible [1, 2]. An important threshold for the tolerable error is 10^{-4} per gate [2, 3] which has been breached for single-qubit gates with a single trapped ion using microwave radiation [4]. However, in a register containing several qubits the manipulation of an individual qubit will, in general, induce errors in the quantum state of all other qubits. This cross-talk may limit the overall fidelity of the quantum register and prevent the application of quantum error correction schemes.

Several methods that allow for addressing of individual ions have been proposed and demonstrated. By utilizing the micromotion in radiofrequency Paul traps, differential Rabi frequencies between trapped ions were induced [5, 6]. Focused laser beams were used to spatially discriminate ions [7], and the use of additional laser beams to reduce cross-talk has been proposed [8].

Static magnetic gradient fields [9] that lead to position dependent Zeeman shifts were employed for addressing [10, 11], and the use of position-dependent light shifts for this purpose was proposed [12] and demonstrated [13]. Also, differential ac Zeeman shifts [5] were employed for addressing ions. An inhomogeneous oscillating field that enables spectral resolution of dressed states was demonstrated [14]. Also, addressing of neutral atoms confined in an optical lattice was recently demonstrated by the use of additional laser fields and microwave radiation [15]. So far, the cross-talk was always either above the error correction threshold or the system has not yet been proven to be scalable beyond two qubits.

Here, we demonstrate an eight-qubit register - a quantum byte - with next-neighbor cross-talk errors on the order of 10^{-5} , about an order of magnitude below the threshold for fault-tolerant quantum computing. The quantum byte is realized using a string of trapped atomic ions confined in a Paul trap. The qubits are encoded in hyperfine levels of $^{171}\text{Yb}^+$ ions exposed to a static magnetic field gradient such that each qubit acquires a specific energy splitting between its physical states, thus allowing to distinguish individual qubits by their resonance frequency. In addition we demonstrate, in a three-qubit quantum register, how by optimally choosing addressing frequency and duration of microwave pulses undesired cross-talk could be reduced even further.

The remainder of this paper is organized as follows: First, the experimental procedure is described that allows to address individual qubits in an eight-qubit quantum register. The ions are addressed in frequency space in the presence of a magnetic gradient field that lifts the qubits' degeneracy. In this quantum register the cross-talk error arises from far-detuned electromagnetic pulses that induce spurious rotations in qubits that are not addressed.

To further study the features of this cross-talk mechanism, we experimentally investigate the effect of far-detuned pulses first using a single hyperfine qubit. By making use of randomized benchmarking techniques we verify the validity of our model that allows to predict the error per single gate as a function of experimental parameters such as the detuning, the power, and the duration of a microwave pulse. Additional sources of error that come along with the application of a single pulse are also briefly discussed.

Then, the central results of this paper are presented. We report on precise measurements of the cross-talk error within the quantum byte using randomized benchmarking. Cross-talk is measured on ion $j = 1, 2, 3, \dots, 8$ when driving single qubit gates on ion $i \neq j$.

In addition, we present a three-qubit quantum register where cross-talk can be further suppressed by appropriately adjusting the qubits' addressing frequencies and the duration of each pulse that induces a gate on the addressed qubit. A brief discussion concludes this paper. The Methods section gives further details on the experimental procedures and data evaluation.

Addressing a quantum byte

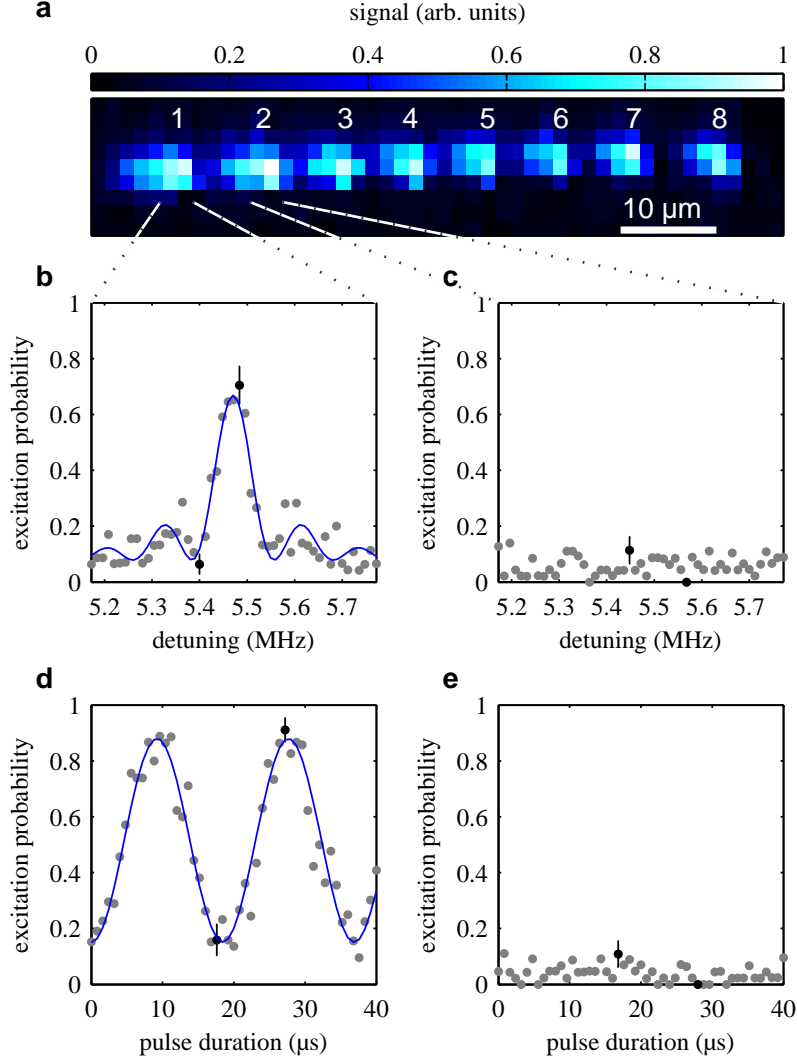


FIG. 1: Addressing of a single qubit within a quantum byte. (a) Spatially resolved resonance fluorescence (near 369 nm) of eight ions held in a linear Paul trap detected by an EMCCD camera. (b) Microwave-optical double resonance spectrum for a fixed pulse length of 10 μs serves for determining the microwave addressing frequency of an individual ion. Here, the state selective resonance fluorescence signal only in the region of ion 1 is considered. (c) Same as in (b), however measuring the signal in the region of next-neighbor ion 2. Non-nearest-neighbor ions (3 through 8) are not affected by manipulating qubit 1 either. Their signal is simultaneously measured but not shown for clarity. (d) Rabi oscillations are only observed in the region of ion 1 when irradiating all ions at the microwave addressing frequency of ion 1. (e) Qubit 2 is left virtually unaffected. Solid lines represent fits of the data. Two points with error bars are displayed in each graph representing typical statistical standard deviations. Each data point represents 50 repetitions.

We realize a quantum register with a chain of thermally excited $^{171}\text{Yb}^+$ ions held in a linear Paul trap. The thermal distribution of vibrational excitation is characterized by the mean vibrational quantum number of the ion crystals axial center-of-mass mode, $\langle n \rangle \approx 150$ [16]. The electronic hyperfine levels of each ion's ground state represent an individual quantum bit: $|0\rangle \equiv |^2S_{1/2}, F=0\rangle$ and $|1\rangle \equiv |^2S_{1/2}, F=1, m_F=+1\rangle$. The energy of state $|1\rangle$ depends on the magnitude of an external magnetic field (Zeeman effect). Therefore, a static magnetic gradient field that is created by permanent magnets included in the trap design lifts the degeneracy between the states $|1\rangle$ of different ions. The frequency differences $\Delta_{i,j}/2\pi = \nu_i - \nu_j$ between individual ions' $|0\rangle \leftrightarrow |1\rangle$ transition frequencies ν_i and ν_j within the chain are given by $\Delta_{i,j} = g_F \mu_B b \delta z_{i,j}/h$, where g_F denotes the Landé g -factor, μ_B the Bohr magneton, b the

magnitude of the magnetic gradient in the axial trap direction, $\delta z_{i,j}$ the spatial separation between ions i and j , and h Planck's constant. The separation $\delta z_{i,j}$ between singly ionized ions is determined by the external axial harmonic trapping potential. In the experiments reported here, this potential is characterized by a secular frequency of $2\pi \times 124$ kHz. As a result, the qubit transition around 12.6 GHz of each ion can be resolved in the frequency domain. A magnetic gradient of 18.8 T/m leads to differences in the addressing frequencies of next-neighbor qubits of a few MHz (details are given in Methods).

The ions are initialized in state $|0\rangle$ through optical pumping. Arbitrary single-qubit gates are implemented by the use of microwave pulses near 12.6 GHz. Conditional two-qubit gates between arbitrary qubits within the register can be implemented employing magnetic gradient induced coupling (MAGIC) within the ion chain [16]. Read-out of the quantum register is achieved by spatially resolved detection of this resonance fluorescence with an EMCCD detector.

We first determine the resonance frequencies of individual qubits within a register of eight qubits by microwave-optical double resonance spectroscopy [Fig. 1 (a)]. After preparing the register in state $|00000000\rangle$, microwave pulses of 10 μ s duration and variable frequency are applied to all ions. Then, all ions are illuminated with detection laser light and spatially resolved resonance fluorescence is observed. The relative frequency of finding a particular ion in state $|1\rangle$ is obtained upon repeating this sequence of microwave and laser pulses for a given microwave frequency [Fig 1 (b) and (c)]. Thus, observation of individual ion excitation reveals this qubit's addressing frequency. Here, the chosen pulse duration that does not match the duration for a π -pulse and the limited detection efficiency yields an excitation probability below unity in Fig 1 (b).

To proof coherent dynamics of a desired single qubit we apply microwave pulses tuned to the respective qubit's addressing frequency while varying the pulse length. We then observe Rabi oscillations of the addressed qubit while the others are virtually left unaffected [Fig. 1 (d) and (e)] (see Methods for a summary of all ions' addressing and Rabi frequencies.) The separation between the qubits' addressing frequencies amounts to a few MHz, and is much larger than the Rabi frequency at which an individual qubit is manipulated (typically $2\pi \times 20$ kHz). The cross-talk originates, therefore, from the effect of far detuned pulses.

If qubit i is resonantly addressed, the excitation probability of qubit j , for $\Omega_j \ll \Delta_{i,j}$, reads

$$C_{i,j} = \sin^2(\pi \Delta_{i,j} \tau) (\Omega_j / \Delta_{i,j})^2 \quad (1)$$

where Ω_j is the Rabi frequency of ion j when exposed to the microwave field, and τ is the duration of the microwave pulse. For typical parameters in our setup the spurious excitation probability is below 10^{-4} for next-neighbor qubits and smaller for non-neighboring ions. The fidelity of the final state of qubit j after its spurious evolution due to one pulse applied to qubit i with respect to the initially prepared state $|0\rangle_j$ is given by $1 - C_{i,j}$ (Methods).

Using the method of randomized benchmarking, we precisely measure the cross-talk within the quantum register by application of random sequences consisting of up to 1250 pulses [18, 19]. The average state fidelity, $\langle F_{i,j} \rangle$ of qubit j after several sequences of N randomly chosen gates applied on qubit i is given by (Methods)

$$\langle F_{i,j} \rangle(N) = \frac{1}{2}(1 + e^{-2C_{i,j}N}). \quad (2)$$

This expression is valid also for the case when a superposition state of qubit j is initially prepared.

Experimentally simulated cross-talk

In this section, before turning to the precise determination of cross-talk in the quantum byte introduced above, we start by investigating, with single-ion experiments, the error induced by far detuned microwave pulses. For this purpose we choose the first order magnetic insensitive levels $|0\rangle$ and $|0'\rangle \equiv |^2S_{1/2}, F=1, m_F=0\rangle$ as qubit states. Microwave pulses driving this resonance are detuned by $\Delta_\pi = 2\pi \times 2$ MHz from the qubit transition – a detuning typical for the quantum byte – and have a variable duration of $7.5\mu\text{s} \leq \tau \leq 8.5\mu\text{s}$ at a Rabi frequency of $2\pi \times 60.8(5)$ kHz. Spurious excitation to the hyperfine states $|^2S_{1/2}F=1, m_F=\pm 1\rangle$ is negligible here, since a bias field of 0.857 mT is applied such that the microwave pulses are detuned by $\Delta_{\sigma+} = -2\pi \times 10$ MHz and $\Delta_{\sigma-} = 2\pi \times 14$ MHz from the magnetic σ transitions.

To probe the off-resonant excitation, a randomized benchmarking protocol is applied [18]. The qubit is initially prepared either in an eigenstate $|\psi\rangle = |0\rangle$, or, by applying a resonant $\pi/2$ -pulse, in a superposition state $|\psi\rangle = 1/\sqrt{2}(|0\rangle + i|0'\rangle)$. We then apply sequences of up to $N = 3000$ detuned pulses where the phase of each pulse is chosen randomly from the set $\{0, \pi/2, \pi, 3\pi/2\}$. We vary the pulse duration (that is kept constant during one sequence) and measure the final state of the qubit. When a superposition state was initially prepared, a second resonant $\pi/2$ -pulse is applied to the qubit after the random pulse sequence in order to map the superposition state back onto an eigenstate before the projective measurement takes place. Figure 2 shows the resulting fidelity $F = \langle \psi | \rho | \psi \rangle$ between the initially prepared state $|\psi\rangle$ and the measured density matrix ρ (see Methods for details).

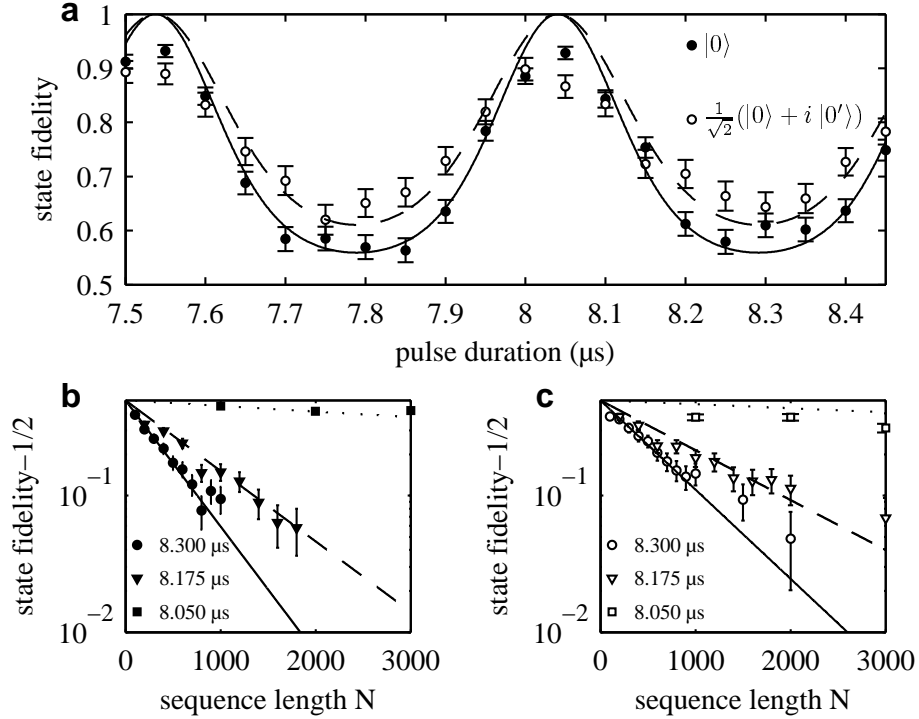


FIG. 2: Features of cross-talk in single ion measurements. (a) State fidelity after 1000 randomized microwave pulses with variable duration for two different input states ($|0\rangle$: filled circles, and $1/\sqrt{2}(|0\rangle + i|0'\rangle)$: open circles). (b) Fidelity of state $|0\rangle$ as a function of the number of applied pulses. The fidelity of the state decreases exponentially with increasing number of pulses. The decay constant depends on the pulse duration. (c) Similar to (b), but with a superposition state prepared initially. Lines represent the expectation from the model. Each data point corresponds to 1000 random sequences. Error bars show standard deviations.

Fig. 2 (a) shows the periodic behavior predicted by the model outlined in the previous section. Fidelity maxima after 1000 detuned pulses appear at 7.55 μs and 8.05 μs and correspond to rotations by an angle of 30π and 32π , respectively, around an axis close to the z direction on the Bloch sphere in an appropriate rotating reference frame. Therefore, after each single pulse the qubit returns to its initial state (modulo a phase $\exp(i\pi)$), while for example pulse durations of 7.8 and 8.3 μs rotate the Bloch vector about 31π and 33π , respectively, which yields the fidelity minima. The effect of detuned pulses also depends on the qubit's state and is smaller for the superposition state [Fig. 2].

In addition, we investigate the rate at which the state fidelity decays during a pulse sequence by varying the sequence length for a given pulse duration. Figure 2 (b) and (c) show the observed decay of the qubit's state fidelity and the prediction from the model (straight lines) for different pulse lengths. Three data sets are shown in each view graph; they are taken for the pulse duration that corresponds to the fidelity maximum, the fidelity minimum, and one value in between, respectively.

For the pulse duration that corresponds to a net rotation of π the state fidelity decays most rapidly while it is better preserved the closer the net rotation is to an even multiple of π . The model (equation (2)) predicts an average change of the fidelity per single pulse of 1.06×10^{-3} (pulse duration of 8.300 μs), 5.3×10^{-4} (pulse duration of 8.175 μs), and 1.8×10^{-4} (pulse duration of 8.050 μs) when state $|0\rangle$ is initially prepared. This is in good agreement with the measured data [Fig. 2]. For the superposition state [Fig. 2 (c)] the fidelity is by a factor of about $\sqrt{2}$ better than when $|0\rangle$ is prepared initially. The reason is that the randomized benchmarking protocol contains microwave pulses with phases that lead to rotations around the x and y axes. If the qubit is, for example, in an eigenstate of x -rotations, it will be less affected by the detuned pulse. Thus, the cross-talk error in the quantum register does not only depend on the relative detuning and the Rabi frequencies but also on the register state (Methods).

Superposition states are affected by the light shift induced by a non-resonant field. We estimate this effect by use of the single-ion quantum lock-in amplifier technique [20]. For next-neighbor qubits the induced error per gate is of the order of 10^{-4} at a Rabi frequency $2\pi \times 60.8(5)$ kHz and a detuning of $2\pi \times 2$ MHz. This effect is systematic and was suppressed here by the use of a spin-echo pulse. During the execution of a quantum algorithm, one can account

TABLE I: Measured cross-talk $\{C_{i,j}\}$ in the quantum byte. The qubits 1 to 8 are addressed (rows) and the resulting cross-talk error ($\times 10^{-5}$) on all the other qubits is observed (columns).

| | | | | | | | |
|----------|----------|----------|----------|----------|----------|----------|----------|
| - | 3.0(9) | 1.9(8) | 2.2(9) | 2.3(9) | 1.0(8) | 0.6(7) | 0.7(7) |
| 3.8(1.4) | - | 4.1(1.1) | 2.3(9) | 2.3(1.1) | 1.6(1.1) | 0.9(0.8) | 0.9(0.9) |
| 2.1(1.0) | 3.7(1.2) | - | 4.5(1.2) | 1.6(7) | 2.1(6) | 0.8(7) | 1.1(6) |
| 0.9(9) | 1.7(6) | 2.7(1.1) | - | 3.1(9) | 0.8(7) | 0.6(6) | 0.6(6) |
| 1.9(9) | 1.6(9) | 3.1(1.0) | 7.6(1.3) | - | 3.1(1.0) | 1.8(9) | 0.5(5) |
| 1.5(5) | 1.2(8) | 1.5(8) | 1.0(8) | 5.5(1.4) | - | 3.6(1.3) | 0.8(8) |
| 0.8(8) | 1.4(8) | 1.5(7) | 1.2(8) | 1.2(8) | 2.9(1.1) | - | 2.6(8) |
| 0.8(6) | 1.1(5) | 0.6(6) | 0.8(8) | 2.5(9) | 1.1(8) | 3.4(1.2) | - |

for it by adjusting the phase of subsequent pulses [5]. In addition to the light shift, the mutual J-coupling changes a superposition state. In the experimental setup used here the next-neighbor coupling strength is about $2\pi \times 50$ Hz [16] which yields, if not compensated for, an induced error per gate of 5×10^{-6} .

Measured cross-talk within quantum registers

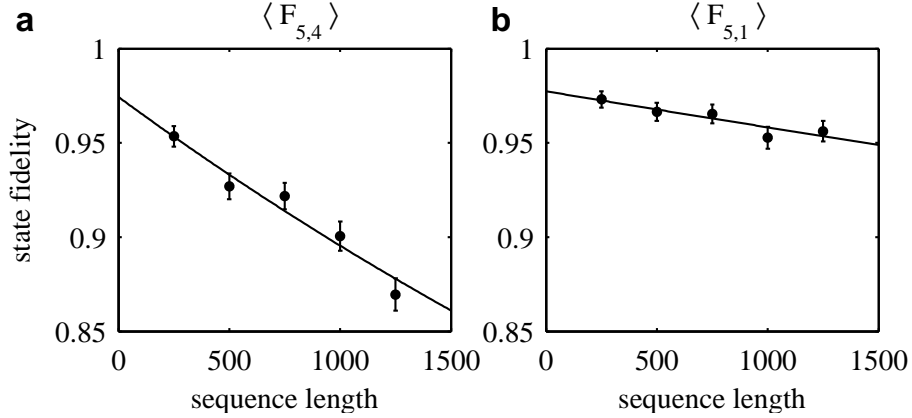


FIG. 3: Exemplary effect of cross-talk within the quantum byte. Qubit 5 is addressed and the fidelity decay of the next-neighbor qubit 4 (a) and the non-next-neighbor qubit 1 (b) is observed. Both qubits' fidelity is initially 0.975(11). The dominant next-neighbor cross-talk of $C_{5,4} = 7.6(1.3) \times 10^{-5}$ causes qubit 4's fidelity to decay faster than that of qubit 1 which is affected by a cross-talk of $C_{5,1} = 1.9(9) \times 10^{-5}$ only. Solid lines are a fit to the data from which the cross-talk is deduced. Each point represents 1600 repetitions. Error bars represent standard deviations.

We now determine the cross-talk within the quantum byte. As before, we apply randomly constructed pulse sequences addressed to one of the qubits within the register and detect the final register state. Each qubit is encoded in states $|0\rangle$ and $|1\rangle$. The experimental procedure to deduce the average cross-talk per single gate is a direct extension of the method applied above. First, the register is initialized in $|00000000\rangle$. Next, a microwave pulse sequence consisting of up to 1250 pulses with randomized phases is applied. The frequency and duration of the pulses are chosen such that they lead to a resonant π pulse addressed to one of the qubits. At the end of the sequence the register is read out. These experimental steps are repeated while the sequence length is varied. The cross-talk induced by randomized pulse sequences causes the non-addressed qubits' states to diffuse on the Bloch sphere. A fit of the fidelity, experimentally determined as a function of N , gives again the average change of the fidelity per single pulse, the cross-talk $C_{i,j}$ (eq. (2)). The model fitted to the data takes into account non-perfect state preparation and detection.

Figure 3 shows some exemplary measurement results. The cross-talk of qubit 4 (a) and 1 (b) are deduced from the data, if qubit 5 is addressed. As one can clearly see the dominant next-neighbor cross-talk causes qubit 4's state fidelity to decay faster than qubit 1's. Recording and analyzing data similar to what is shown in Fig. 3 for each pair of qubits allows to construct the cross-talk matrix $\{C_{i,j}\}$, $i \neq j$. We summarize the cross-talk within the quantum byte in table I. Clearly, next-neighbor cross-talk dominates.

One notices that the non-next-neighbor cross-talk, if qubit 1 or 2 is addressed is bigger than if, in contrast, qubit

7 or 8 is addressed. The reason for this, at first sight unexpected asymmetry, is the existence of the resonance $|0\rangle \leftrightarrow |0'\rangle$. This resonance is insensitive to the magnetic field to first order, and thus occurs for all ions at about the same frequency. An ion in qubit state $|0\rangle$ can, therefore, be spuriously excited to qubit state $|1\rangle$, or to state $|0'\rangle$. Both excitations lead to a reduction of the state fidelity of the qubit $\{|0\rangle, |1\rangle\}$. In the experiments reported here, the difference between the addressing frequency of ion 1, ν_1 and the frequency of resonance $|0\rangle \leftrightarrow |0'\rangle$ is 5.5 MHz, determined by a constant bias field of 0.390 mT, while $\nu_1 - \nu_4 = -6.3$ MHz and $\nu_1 - \nu_8 = -14.4$ MHz, respectively. Therefore, the excitation on the common resonance ($|0\rangle - |0'\rangle$) is, for this choice of a bias field and the location of the point where the gradient field vanishes, the dominant effect that leads to reduction of the state fidelity.

Importantly, the experimentally determined cross-talk on the order of 10^{-5} , as shown in Fig. 3 and Table I, includes *any* possible source of cross-talk, with the main contribution arising from non-resonant excitation.

The periodicity of the average cross-talk error per single gate, as shown in figure 2 (a), can be exploited to create quantum registers in which the total remaining cross-talk due to non-resonant excitation ideally vanishes or, at least, is efficiently suppressed. The key idea is a gate applied to one of the qubits that leads to rotations of all non-addressed qubits' Bloch vectors by about an integer multiple of 2π . Hence, their states will effectively not change (modulo a known phase). This can be achieved, for example, in a chain of ions in which the detunings of all next-neighbor ions and the Rabi frequencies are equal ($\tilde{\Delta} \equiv \Delta_{i,i+1}$, $i = 1, \dots, N-1$ and $\Omega_i \equiv \tilde{\Omega}$, $i = 1, \dots, N$ where N is the number of ions). A pulse that effectively rotates a non-addressed next-neighbor qubit around 2π will, to good approximation, also rotate all other non-addressed qubits by the same net rotation as well.

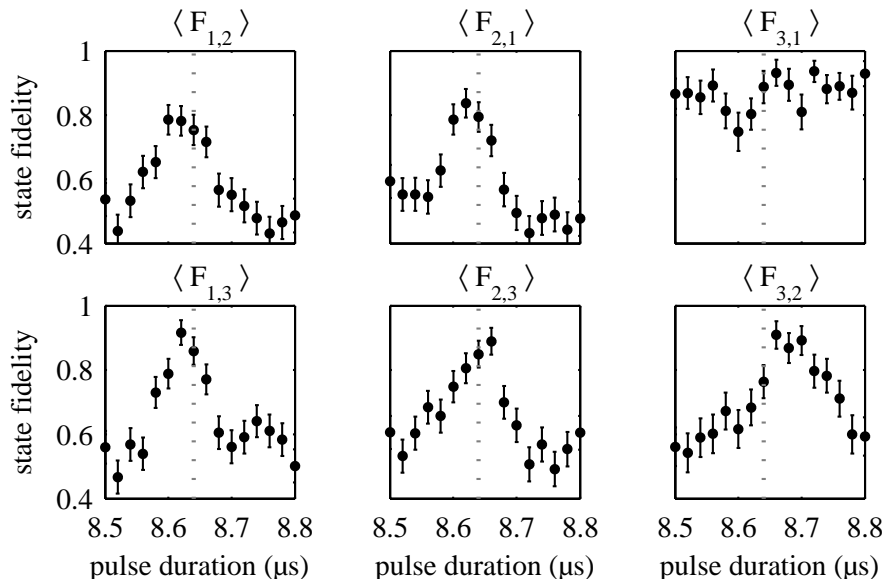


FIG. 4: Estimating the optimal pulse duration for a three-qubit register. Random sequences of 2000 pulses are addressed to each of the qubits resonantly and the fidelity decay of the other qubits is observed. The optimal pulse duration of $8.64 \mu\text{s}$ (emphasized by a dotted line) yields a preserved state fidelity on all non-addressed qubits. Each data point corresponds to 350 repetitions. Error bars represent one standard deviation.

We realize such an optimized quantum register with three ions. The constant magnetic gradient yields the same next-neighbor separation in the frequency domain ($\tilde{\Delta} = \Delta_{1,2} = \Delta_{2,3}$). A magnetic bias field of about 0.240 mT results in the same frequency difference between the addressing frequency of ion 1 and the frequency of the resonance $|0\rangle \leftrightarrow |0'\rangle$ ($\tilde{\Delta} = 2\pi \times 3.358(3)$ MHz). In this configuration, the magnetic σ^- transition of each ion is set apart by an integer multiple of $\tilde{\Delta}$ from the ions' addressing frequencies.

We first estimate the pulse duration that suppresses the cross-talk, again by application of randomized pulse sequences. The sequence length is kept constant at 2000 pulses while the pulse duration is varied. As is evident in figure 4, a pulse duration of $\tau_{\text{optimal}} = 8.64 \mu\text{s}$ results in highly preserved state fidelities for all non-addressed qubits after the application of 2000 pulses. The difference in the behavior depending on whether qubit 1 or qubit 3 is addressed is, again (as outlined above for the case of the quantum byte), caused by the presence of the resonance $|0\rangle \leftrightarrow |0'\rangle$ that occurs at nearly the same frequency for all three ions. The addressing frequency of qubit 1 is closer to this resonance than to the addressing frequency of qubit 3. This is evident in Fig. 4 where the fidelity decay shows a slower periodicity that is due to a detuning of $\tilde{\Delta}$ only.

TABLE II: Measured cross-talk $C_{i,j}$ in the optimized three-qubit quantum register. The qubits are addressed (rows) and the resulting cross-talk error ($\times 10^{-5}$) on the two others is observed (columns).

| | | |
|--------|-------|-------|
| - | 23(5) | 6(1) |
| 8(2) | - | 10(2) |
| 2.7(3) | 6(1) | - |

The Rabi frequency ($\tilde{\Omega} = 2\pi \times 57.9$ kHz) is adjusted such that the pulse duration τ_{optimal} results in π -pulses on the addressed qubit. According to the experimental procedure described above for the case of a quantum byte, we measure the cross-talk within the optimized three-qubit register by application of up to 5000 pulses. The results are summarized in Table II. Again, the resonance $|0\rangle \leftrightarrow |0'\rangle$ is responsible for the increased cross-talk on qubit 2, if qubit 1 is addressed.

The cross-talk is below the prediction for next-neighbor cross-talk of 3×10^{-4} according to eq. 1 at a Rabi frequency of $2\pi \times 57.9$ kHz that is about three times higher than what was used for addressing the quantum byte. This clearly demonstrates the improvement in cross-talk achieved by letting the non-addressed qubits rotate approximately multiples of 2π .

Residual cross-talk arises not only because of the possible excitation of the ions' $|0\rangle \leftrightarrow |0'\rangle$ resonance, but also because of addressing frequencies drifting during the experiment [21] and through excitation of motional sidebands. Here, the sidebands of the common mode are ± 124 kHz apart from the qubits addressing frequencies [16]. The Rabi frequencies on the red and blue sideband transition are proportional to \sqrt{n} and $\sqrt{n+1}$, where n denotes the phonon occupation number of the mode. In the experiments described here, the ions are thermally excited with a phonon occupation of $\langle n \rangle \approx 150$. Since cross-talk is proportional to the square of the transition's Rabi frequency, one can suppress it by further cooling the ions. The measured values of cross-talk shown in Table II include all sources of error.

The method described above can be extended to larger registers in systems with either a spatially varying magnetic gradient or systems that allow either anharmonic trap potentials or local potentials as for example segmented micro traps [22–25]. In these systems the qubits' addressing frequencies and pulse durations may be adjusted appropriately.

Discussion

In conclusion, we investigate and characterize cross-talk mechanisms in quantum registers with trapped ions. We experimentally quantify the cross-talk induced by a resonant π -pulse addressed to a particular qubit by directly measuring the average excitation of all other qubits after up to 1250 pulses. For the quantum byte, the next-neighbor cross-talk is of order 10^{-5} . The direct measurement of cross-talk takes into account all possible sources of error. Non-resonant excitation was identified as the main source.

In a three-qubit register a method for further reducing cross-talk is experimentally characterized. This method is based on appropriately adjusting addressing frequencies and pulse durations and, again, breaches the threshold for fault-tolerant quantum computing even if the single qubit gates are applied at higher Rabi frequencies of about $2\pi \times 60$ kHz.

Spurious excitation on undesired hyperfine transitions can be further suppressed by either increasing the magnetic bias field or by adjusting the microwave polarization. For $\pi/2$ -rotations around the $\pm x$ and $\pm y$ axes that together with π -pulses generate the single-qubit Clifford group, the cross-talk mechanisms are the same as for π -pulses investigated in this study. The pulse duration is halved but the cross-talk is still of the same order of magnitude. Systematic rotations around the qubits' z axes do not contribute to cross-talk, since they can be compensated by adjusting the relative phase of consecutive microwave pulses and do not require the application of additional pulses. For example, the microwave light shift that results in a rotation around the z axis leads to a systematic error that can be accounted for [5].

Acknowledgement

We acknowledge funding by the Bundesministerium für Bildung und Forschung (FK 01BQ1012), from the European Community's Seventh Framework Programme (FP7/2007-2013) under Grant Agreement No. 270843 (iQIT), and from Deutsche Forschungsgemeinschaft.

Methods

Cross-talk for far detuned pulses

The cross-talk in the investigated addressing scheme is mainly due to the effect of far detuned pulses of coherent electromagnetic radiation. While one qubit i is resonantly addressed at microwave frequency ω_i , the other qubits $j \neq i$ are exposed to non-resonant radiation at frequency $\omega_i + \Delta_{i,j}$. We are interested in describing the spurious dynamics of a given qubit j while qubit i is addressed.

First we concisely review relevant features of the quantum dynamics of a single qubit under irradiation with microwave radiation. The time evolution of qubit j is conveniently described in a reference frame that rotates at frequency ω_i . Specifically, the evolution of qubit j while irradiated by microwave radiation is described by a rotation $R_{\vec{n}}(\theta) = \exp(-i\theta/2\vec{n} \cdot \vec{\sigma}) \in \text{SU}(2)$ around unit vector \vec{n} by an angle $\theta = \Omega_R\tau$, where $\Omega_R = \sqrt{\Omega_i^2 + \Delta_{i,j}^2}$ denotes the generalized Rabi frequency, $\Delta_{i,j}$ is the detuning, τ is the duration of a square pulse, and $\vec{\sigma} = (\sigma_x, \sigma_y, \sigma_z)$ with the Pauli matrices σ_i . The magnitude of the component of \vec{n} in the xy -plane of the Bloch sphere, $n_{\perp} = \Omega_i/\Omega_R$, and in the z -direction, $n_z = \Delta_{i,j}/\Omega_R$. Thus, for far detuned pulses, the qubit's dynamics on the Bloch sphere while exposed to a far detuned pulse is described by a rotation around an axis that is nearly parallel to the z axis.

In a quantum register where all qubits have been prepared in their ground state $|0\rangle$ the addressing of a single qubit i for the duration τ will spuriously excite all other qubits $j \neq i$. The induced cross-talk error per single pulse on qubit j is

$$\begin{aligned} C_{i,j} &= |\langle 1 | R_{\vec{n}}(\theta) | 0 \rangle|^2 \\ &= (\Omega_i/\Omega_R)^2 \sin^2(\Omega_R\tau/2). \end{aligned} \quad (3)$$

For far detuned pulses ($\Delta \gg \Omega$)

$$C_{i,j} \approx (\Omega_i/\Delta_{i,j})^2 \sin(\Delta_{i,j}\tau). \quad (4)$$

Thus, the maximal spurious excitation probability for a single pulse is $(\Omega_i/\Delta_{i,j})^2$. For a pulse duration of $\tau = 2\pi/\Delta_{i,j}$ the qubit's Bloch vector is rotated by an angle of 2π and hence leaves the qubit excitation probability effectively unchanged. One can take advantage of this periodicity to further lower the cross talk error (compare Figs. 4).

When a superposition state of qubit j is prepared initially (Fig. 2 (a) and (c)), the effect of detuned pulses on this qubit is probed employing a Ramsey-type experiment. After preparing the qubit in $|0\rangle$ a resonant $\pi/2$ -pulse is applied on the $|0\rangle - |0'\rangle$ resonance to drive qubit j into a superposition state before qubit i is addressed. The second $\pi/2$ -pulse would ideally excite qubit state into state $|1\rangle$, if qubit j were not affected by the non-resonant pulses addressing qubit i . The deviation from full population transfer is given by equation 4. Rotations around the z -axis are compensated by a resonant π -pulse applied to qubit j in between the two $\pi/2$ -pulses.

Effect of randomized pulse sequences

For the typical parameters in our setup ($\Omega = 2\pi \times 20$ kHz and $\Delta_{i,i+1} = 2\pi \times 2$ MHz) the cross-talk error (4) is of order 10^{-5} which is much smaller than typical state preparation and detection errors. To measure such a small effect we make use of randomized gate sequences [18]. From the application of several gates and the observation of accumulating errors we deduce the error per single gate. For our measurements of the cross-talk error one can visualize the method by making use of the concept of diffusion as will be described below.

According to the discussion above a single microwave pulse addressed to qubit i will rotate the state vectors of the qubits j about an axis defined by the phase of the pulse and the mutual detunings $\Delta_{i,j}$. A sequence of several pulses with randomly chosen phases will therefore result in a random walks of the qubits j on their Bloch spheres. In the applied randomized benchmarking protocol the phase and therefore the nutation axis of each pulse is chosen randomly from $\{0, \pi/2, \pi, 3\pi/2\}$ in every single realization of the sequences. All the pulses that are applied during our study are rectangular pulses and the duty cycle of each sequence is 50%.

If the random paths of several sequences are taken into account the average position of the final state of each qubit j will be spread over the Bloch sphere which can be described, in general, by the diffusion equation

$$\partial_t \phi_{i,j}(\vec{r}, t) = D \nabla^2 \phi_{i,j}(\vec{r}, t). \quad (5)$$

Here, $\phi_{i,j}(\vec{r}, t)$ denotes the probability density function of finding qubit j 's state vector at the location \vec{r} on its Bloch sphere at time t , and D denotes the diffusion constant.

Due to the symmetry of the problem we can simplify it to the one-dimensional case where the single spatial coordinate x denotes the distance from the initially prepared state vector on the Bloch sphere.

We solve the problem for the state vector being either an energy eigenstate or a superposition state. For both cases a corresponding polar coordinate system is defined such that the initial state is found at $x_0 = \pi$.

This equation is solved for both cases by

$$\phi_{i,j}(x, t) = \frac{1}{\pi} \sum_{m=0}^{\infty} e^{-\lambda_{i,j}(m)t} (-1)^m \cos(mx) - \frac{1}{2\pi}, \quad (6)$$

where $\lambda_{i,j}(m) = D/m^2$.

The solution fulfills the periodic boundary conditions of the qubits topology and the initial condition. With knowledge of the probability density, one can calculate the time-dependent state fidelity with the initial state:

$$\begin{aligned} \langle F_{i,j}(t) \rangle &= \int_0^{2\pi} dx \phi_{i,j}(x, t) F(x), \\ &= \int_0^{2\pi} dx \phi_{i,j}(x, t) \frac{1}{2} (1 - \cos(x)), \\ &= \frac{1}{2} (1 + e^{-\lambda_{i,j}(1)t}). \end{aligned} \quad (7)$$

The diffusion is driven by cross-talk errors induced by pulse sequences addressed to qubit i . The average fidelity of qubit j after qubit i was addressed with N random pulses is related to the error probability per single gate $C_{i,j}$ by

$$\langle F_{i,j}(N) \rangle = \frac{1}{2} (1 + e^{-2C_{i,j}N}). \quad (8)$$

The cross-talk $C_{i,j}$ per single gate is deduced from measuring the fidelity $\langle F_{i,j}(N) \rangle$ of a non-addressed qubit while the randomized benchmarking protocol is applied to qubit i . The model fitted to the data reads

$$f(p_0, p_1, N) = 1/2 \times (1 + (2p_0 - 1) \exp(-2/p_1 \times N)). \quad (9)$$

Here, the free fit parameter p_0 describes non-perfect state preparation and detection, p_1 describes the decay of fidelity (from which the cross-talk error is deduced) and N is the number of pulses applied to qubit i .

Estimating state fidelities

We experimentally deduce the cross-talk errors in the quantum register by observing the state fidelity of the non-addressed qubits $j \neq i$. This fidelity decays during the application of the randomized benchmarking protocol addressed to qubit i (eq. (8)). The fidelity

$$\langle F_{i,j} \rangle = \langle \psi_j | \rho_{i,j} | \psi_j \rangle. \quad (10)$$

Here, $\rho_{i,j}$ denotes the final state density matrix of qubit j after having been exposed to random sequences of detuned pulses addressed to qubit i , and $|\psi_j\rangle$ is the initial state of qubit j .

With respect to the initially prepared ground state, $|0\rangle$, the fidelity of the final state is

$$\langle F_{i,j} \rangle = \langle 0 | \rho_{i,j} | 0 \rangle = \rho_{i,j}^{00}. \quad (11)$$

We can, therefore, determine the average fidelity of qubit j by measuring the excitation probability (or rather relative frequencies) of qubit j into $|1\rangle$, $P_{i,j}$, after the randomized benchmarking sequence has been addressed to qubit i , and

$$\langle F_{i,j} \rangle = 1 - P_{i,j}. \quad (12)$$

With respect to the superposition state $\frac{1}{\sqrt{2}}(|0\rangle + e^{i\pi/2}|1\rangle)$ the fidelity (10) reads

$$\langle F_{i,j} \rangle = \frac{1}{2} (1 + 2|\rho_{i,j}^{01}|). \quad (13)$$

The probability $P_{i,j}$ to find qubit j in state $|1\rangle$ after the application of the Ramsey-type pulse sequence mentioned above (the relative phase between the $\pi/2$ - pulses is not varied) is

$$P_{i,j} = \frac{1}{2} (1 + 2|\rho_j^{01}|) = F_{i,j}. \quad (14)$$

TABLE III: Addressing of the quantum byte. The first column lists the ion's number, the second column the qubits' resonance frequencies, and the third column the Rabi frequencies at which single qubit gates are applied. These results are obtained employing microwave-optical double resonance spectroscopy (Fig. 1). The variation in Rabi frequencies in the eight-ion experiment reported here is due to an inhomogeneous static magnetic field perpendicular to the trap axis. Ion $i = 1, 2, 3, \dots, 8$ was addressed using a Rabi frequency $\Omega_i = 2\pi \times 20$ kHz. The perpendicular magnetic field component was nulled for the experiments demonstrating the optimized three-qubit register.

| i | ν_i (GHz) | $\Omega/2\pi$ (kHz) |
|-----|---------------|---------------------|
| 1 | 12.648298(3) | 54.1(5) |
| 2 | 12.650634(3) | 46.7(6) |
| 3 | 12.652658(4) | 43.5(6) |
| 4 | 12.654523(4) | 40.0(7) |
| 5 | 12.656375(9) | 38.2(1.2) |
| 6 | 12.658282(9) | 34.4(6) |
| 7 | 12.660302(9) | 30.7(8) |
| 8 | 12.662694(11) | 28.5(8) |

Experimental procedures

We briefly describe the experimental procedure that was performed to experimentally deduce the cross-talk errors $C_{i,j}$. The results for the input state $|0\rangle$ (Fig. 2 (a) and (b), Fig. 3 (a) and (b) and Fig. 4) are obtained by the following experimental procedure. The ions are initialized in state $|0\rangle$ through optical pumping on the optical transition $|^2S_{1/2}, F=1\rangle \leftrightarrow |^2P_{1/2}, F=1\rangle$ using laser light near 369 nm. Doppler cooling of the ion chain and state selective detection of the ions' qubit state is achieved by driving the transition $|^2S_{1/2}, F=1\rangle \leftrightarrow |^2P_{1/2}, F=0\rangle$ again with laser light near 369 nm. Optical pumping into the metastable $D_{3/2}$ state is prevented by illuminating the ions with laser light near 935 nm [17]. These two light fields are referred to as detection laser light in this paper. Then, a randomized microwave pulse sequence (described above) is applied before read-out of the quantum register is achieved by spatially resolved detection of resonance fluorescence using an EMCCD detector. Alternatively, a photomultiplier may be used to detect the overall fluorescence. These steps are repeated in order to obtain statistical significance. From the probability of finding an ion in its bright state the fidelity is deduced (see above).

Table III lists the experimentally determined qubit resonance- and Rabi frequencies for the quantum byte used here.

-
- [1] A. M. Steane, Phys. Rev. Lett. **77**, 793 (1996).
 - [2] J. Preskill, Proc. R. Soc. London, Ser. A **454**, 385 (1998).
 - [3] E. Knill, Nature (London) **463**, 441 (2010).
 - [4] K. R. Brown, A. C. Wilson, Y. Colombe, C. Ospelkaus, A. M. Meier, E. Knill, D. Leibfried, and D. J. Wineland, Phys. Rev. A **84**, 030303 (2011).
 - [5] U. Warring, C. Ospelkaus, Y. Colombe, R. Jrdens, D. Leibfried and D. J. Wineland, Phys. Rev. Lett. **110**, 173002 (2013).
 - [6] Q. A. Turchette, C. S. Wood, B. E. King, C. J. Myatt, D. Leibfried, W. M. Itano, C. Monroe, and D. J. Wineland, Phys. Rev. Lett. **81**, 3631-3634 (1998).
 - [7] H. C. Nägerl, D. Leibfried, H. Rohde, G. Thalhammer, J. Eschner, F. Schmidt-Kaler, and R. Blatt, Phys. Rev. A **60**, 145 (1999).
 - [8] C. Shen, Z. X. Gong, and L. M. Duan, Phys. Rev. A **88**, 052325 (2013).
 - [9] F. Mintert and Ch. Wunderlich, Phys. Rev. Lett. **87**, 257904 (2001).
 - [10] S. X. Wang, J. Labaziewicz, Y. Ge, R. Shewmon, and I. L. Chuang, Appl. Phys. Lett. **94**, 094103 (2009).
 - [11] M. Johanning, A. Braun, N. Timoney, V. Elman, W. Neuhauser and Ch. Wunderlich, Phys. Rev. Lett. **102**, 073004 (2009).
 - [12] P. Staunum and M. Drewsen, Phys. Rev. A **66**, 040302 (2002).
 - [13] P. C. Haljan, P. J. Lee, K-A. Brickmann, M. Acton, L. Deslauriers, and C. Monroe, Phys. Rev. A **72**, 062316 (2005).
 - [14] N. Navon, S. Kotler, N. Akerman, Y. Glickman, I. Almog, and R. Ozeri, Phys. Rev. Lett. **111**, 073001 (2013).
 - [15] J. H. Lee, E. Montano, I. H. Deutsch, and P. S. Jessen, Nat. Commun. **4**, 2027 (2013).
 - [16] A. Khromova, Ch. Piltz, B. Scharfenberger, T. F. Gloger, M. Johanning, A. F. Varón and Ch. Wunderlich, Phys. Rev. Lett. **108**, 220502 (2012).
 - [17] Chr. Balzer, A. Braun, T. Hannemann, Chr. Paape, M. Ettler, W. Neuhauser, and Chr. Wunderlich, Phys. Rev. A **73**, 041407 (2006).
 - [18] E. Knill, D. Leibfried, R. Reichle, J. Britton, R. B. Blakestad, J. D. Jost, C. Langer, R. Ozeri, S. Seidelin, and D. J. Wineland, Phys. Rev. A **77**, 012307 (2008).

- [19] J. M. Gambetta, A. D. Córcoles, S. T. Merkel, B. R. Johnson, J. A. Smolin, J. M. Chow, C. A. Ryan, Chad Rigetti, S. Poletto, T. A. Ohki, M. B. Ketchen, and M. Steffen, *Phys. Rev. Lett.* **109**, 240524 (2012).
- [20] S. Kotler, N. Akerman, Y. Glickman, A. Keselman and R. Ozeri, *Nature (London)* **473**, 61 (2011).
- [21] Ch. Piltz, B. Scharfenberger, A. Khromova, A. F. Varón, and Ch. Wunderlich, *Phys. Rev. Lett.* **110**, 200501 (2013).
- [22] D. Kaufmann, T. Collath, M. T. Baig, P. Kaufmann, E. Asenwar, M. Johanning and Ch. Wunderlich, *Appl. Phys. B* **107**, 935-943 (2012).
- [23] D. Mc Hugh and J. Twamley, *Phys. Rev. A* **71**, 012315 (2005).
- [24] G.-D. Lin, S.-L. Zhu, R. Islam, K. Kim, M.-S. Chang, S. Korenblit, C. Monroe and L.-M. Duan, *EPL*, **86**, 60004 (2009).
- [25] P. J. Kunert, D. Georgen, L. Bogunia, M. T. Baig, M. A. Baggash, M. Johanning, and Ch. Wunderlich, *Appl. Phys. B* **114**, 27-36 (2014).